DALTON
FULL PAPER

Two novel anion cluster compounds with a planar 'open' structure $[Et_4N]_2[MS_4Cu_4(SCN)_4(2\text{-pic})_4]$ (M = W, Mo; 2-pic = 2-methylpyridine): synthesis, structural characterization, nonlinear response and large optical limiting properties

Chi Zhang,[a] Yinglin Song,[b] Guocheng Jin,[a] Guangyu Fang,[b] Yuxiao Wang,[b] S. Shanmuga Sundara Raj,[c] Hoong-Kun Fun †[c] and Xinquan Xin *[a]

[a] *State Key Laboratory of Coordination Chemistry, Department of Chemistry, Nanjing University, Nanjing 210093, P. R. China*
[b] *Physical Department, Harbin Institute of Technology, Harbin 150001, P. R. China*
[c] *X-Ray Crystallography Unit, School of Physics, Universiti Sains Malaysia 11800, USM, Penang, Malaysia*

Received 8th December 1999, Accepted 29th February 2000
Published on the Web 30th March 2000

The title compounds $[Et_4N]_2[MS_4Cu_4(SCN)_4(2\text{-pic})_4]$ (M = W **1**, Mo **2**) have been synthesized by the reaction of $(Et_4N)_2MS_4$, Cu(SCN) and 2-picoline (2-pic, 2-methylpyridine). Single crystal X-ray diffraction data show that the anion clusters $[MS_4Cu_4(SCN)_4(2\text{-pic})_4]^{2-}$ have the planar 'open' structure with four Cu atoms in three kinds of coordination modes. Nonlinear optical properties of these two clusters are investigated with a 8 ns pulsed laser at 532 nm. The two clusters exhibit large optical limiting performance, with limiting threshold values of 0.3 J cm^{-2} for **1**, 0.5 J cm^{-2} for **2**, and self-defocusing effects, effective nonlinear refractive index $n_2 = -6.84 \times 10^{-12}$ esu (esu = 7.162×10^{13} m^5 v^{-2}) **1** and $n_2 = -8.48 \times 10^{-12}$ esu **2** respectively. Both compounds show reverse saturable absorption: $\alpha_2 = 3.1 \times 10^{-6}$ m W^{-1} for **1** and $\alpha_2 = 3.2 \times 10^{-6}$ m W^{-1} for **2** in 6.98×10^{-4} mol dm^{-3} and 7.44×10^{-4} mol dm^{-3} DMF solution respectively. The corresponding effective NLO susceptibilities $\chi^{(3)}$ are 6.5×10^{-8} esu **1** and 8.9×10^{-8} esu **2** while the corresponding hyperpolarizabilities ($\gamma_{(1)} = 9.42 \times 10^{-32}$ esu and $\gamma_{(2)} = 1.29 \times 10^{-31}$ esu) are also reported.

Introduction

Much effort has been directed at exploring new active research frontiers of third-order optical nonlinearity, not only from the perspective of understanding nonlinear optical (NLO) phenomena[1,2] but also from their potential technological applications, such as in the development of optical limiting (OL) devices designed to protect sensitive optical sensors including human eyes from intense laser radiation.[3–5] These 'optical limiters' mainly rely on gas, liquid or solid state nonlinear optical material, whose absorption is weak at low incident light energy but becomes extremely strong under intense light radiation. Such nonlinear absorption behavior is referred to as reverse saturable absorption (RSA), in contrast to saturable absorption found in most materials.

The RSA process was first observed by Giuliano and Hess[6] in dye molecules such as Sudanschwartz-B and Indanthrone. Since then, a number of compounds including phthalocyanine,[4a] metallophthalocyanine,[7] iron tricobalt cluster,[8] fullerenes C_{60}[3a,c,9] and King's complex[10] have been found to possess such a property. Physically, RSA occurs as a consequence of the excited-state absorption cross-section being larger than that of the ground state. As the optical excitation intensity increases, more molecules are promoted to the excited state, thus leading to higher absorption at intense light excitation. Because the RSA process involves electronic transition and a long-life triplet state, the long life time typically associated with the triplet state ensures that the material response is relatively pulse-width insensitive over a wide range of pulse durations. Moreover, many of these molecules have a broad linear absorption, resulting in a broadband limiting response. These advantages make RSA extremely attractive for use in broadband OL of pulsed lasers.

Heterothiometallic cluster compounds have received a great deal of attention because they also possess strong RSA and rather diverse combinations of NLO effects.[11–19] In order to expand this research further, in this article, we report the observation of the RSA effects of two clusters $[Et_4N]_2[MS_4Cu_4(SCN)_4(2\text{-pic})_4]$ (M = W **1**, Mo **2**; 2-pic = 2-methylpyridine (2-picoline)) as well as their nonlinear refraction and their large OL properties. Besides, to our knowledge, synthesis and structure characterization of these two novel pyridine-derivative-containing anionic clusters having a pentanuclear 'open' structure with four Cu atoms in three kinds of coordination mode are reported for the first time.

Experimental

General

All reactions and manipulations were conducted using standard Schlenk techniques under an atmosphere of nitrogen. The starting materials $(Et_4N)_2MS_4$ (M = W, Mo) and Cu(SCN) were obtained according to the literature.[20,21] The solvents were carefully dried and distilled prior to use and other chemicals were generally used as commercially available.

Preparations

$[Et_4N]_2[WS_4Cu_4(SCN)_4(2\text{-pic})_4]$ 1. Cu(SCN) (2 mmol, 0.12 g) was added to 2-picoline (40 cm^3) and the solution was stirred

† To whom correspondence regarding the crystal structure determination should be addressed.

DOI: 10.1039/a909656f

Table 1 Crystal data for $[Et_4N]_2[MS_4Cu_4(SCN)_4(2\text{-pic})_4]$ (M = W **1** or Mo **2**)

	1	**2**
Chemical formula	$C_{44}H_{68}N_{10}WCu_4S_8$	$C_{44}H_{68}N_{10}MoCu_4S_8$
Formula weight	1431.57	1343.66
Crystal system	Tetragonal	Tetragonal
Space group	$P4_32_12$	$P4_32_12$
μ(Mo-Kα)/mm^{-1}	3.556	1.876
a/Å	14.69820(10)	14.6884(3)
b/Å	14.67930(10)	14.6881(2)
c/Å	28.3219(3)	28.3778(6)
V/Å^3	6110.71(9)	6122.4(2)
Z	4	4
T/K	293(2)	293(2)
Reflections collected/ unique	26399/3999 [R_{int} = 0.0353]	26338/4000 [R_{int} = 0.0989]
Final R indices [$I > 2\sigma(I)$]	$R1$ = 0.0202, wR = 0.0519	$R1$ = 0.0452, wR = 0.0848

for *ca.* 5 min at room temperature. The system changed from colorless to yellow and the Cu(SCN) dissolved totally. Then $(Et_4N)_2WS_4$ (0.5 mmol, 0.286 g) was added. The reacting system immediately turned deep red and was stirred for an additional 10 min. The resulting solution was subsequently filtered to afford a deep red filtrate. Red crystals were obtained after several days by layering the filtrate with i-PrOH. Yield: 0.662 g (92.5%). Found: C, 37.03; H, 4.92; N, 9.95%. Anal. Calcd. for $C_{44}H_{68}N_{10}WCu_4S_8$: C, 36.91; H, 4.79; N, 9.79%. IR (KBr pellets, cm^{-1}): 2087.9(vs), 1602.5(s), 1482.9(vs), 753.7(vs), 439.8(vs).

$[Et_4N]_2[MoS_4Cu_4(SCN)_4(2\text{-pic})_4]$ 2. The same procedure as in the preparation of cluster **1** was employed to synthesize the cluster **2** except using $(Et_4N)_2MoS_4$ (0.5 mmol, 0.243 g) instead of $(Et_4N)_2WS_4$ (0.5 mmol). Black-red crystals were obtained. Yield: 0.611 g (91.0%). Found: C, 39.56; H, 5.44; N, 10.38%. Anal. Calcd. for $C_{44}H_{68}N_{10}MoCu_4S_8$: C, 39.33; H, 5.10; N, 10.42%. IR (KBr pellets, cm^{-1}): 2088.3(vs), 1602.7(s), 1483.1(vs), 754.1(vs), 450.6(vs).

Crystal structure determinations

A well-developed single crystal of cluster **1** or **2** with suitable dimensions was mounted on a glass fiber and diffraction data were collected at 20 ± 2 °C on a Siemens Smart CCD area-detecting diffractometer in the range $3.12 < 2\theta < 45°$ by using an ω-scan technique. The data reductions were performed on a Silicon Graphics Indy workstation with Smart-CCD software. The structures were solved by direct methods and refined by full-matrix least-squares on F^2 using the SHELXTL-PC package of crystallographic software.[22] All non-hydrogen atoms were refined anisotropically. The hydrogen atoms were generated and included in the structure factor calculations with assigned isotropic thermal parameters but were not refined. The Flack parameters of these two clusters are −0.009(6) **1** and 0.02(2) **2**, respectively. The data processing and structure refinement parameters are listed in Table 1.

CCDC reference number 186/1877.

See http://www.rsc.org/suppdata/dt/a9/a909656f/ for crystallographic files in .cif format.

Other characteristic measurements

Elemental analysis for carbon, hydrogen and nitrogen were performed on a Perkin-Elmer 240C elemental analyzer. Infrared spectra were recorded with a Nicolet FT-170SX Fourier transform spectrometer (KBr pellets). The electronic spectra were measured on a Shimadzu UV-3100 spectrophotometer.

Optical measurements

A DMF solution of the cluster **1** or **2** was placed in a 5 mm quartz cuvette for optical limiting properties measurements which were performed with linearly polarized 8 ns pulses at 532 nm generated from a Q-switched frequency-doubled Nd:YAG laser. Clusters **1** and **2** are stable toward air and laser light under experimental conditions. The spatial profiles of the optical pulses were of nearly Gaussian transverse mode. The pulsed laser was focused onto the sample cell with a 15 cm focal length focusing mirror. The spot radius of the laser beam was measured to be 55 μm (half-width at 1/e^2 maximum). The input and output pulse energies were measured simultaneously by precision laser detectors (Rjp-735 energy probes) while the incident pulse energy was varied by a Newport Com. Attenuator. The interval between the laser pulses was chosen to be 1 s to avoid the influence of thermal and long-term effects.

The effective third-order NLO absorptive and refractive properties of clusters **1** and **2** were recorded by moving the samples along the axis of the incident laser beam (Z-direction) with respect to the focal point instead of being positioned at its focal point, and an identical setup was adopted in the experiments to measure the Z-scan data. An aperture of 0.5 mm radius was placed in front of the detector to assist the measurement of the nonlinear optical absorption and self-defocusing effect.

Results and discussion

Synthetic reactions

The synthetic route to compounds **1** or **2** was designed based on the ligand-exchange or ligand-redistribution reaction to obtain mixed-ligand clusters in a two-step reaction. At the first step, the copper complex including mixed-ligands was pre-synthesized as the intermediate product, which need not be isolated from the reaction system. In our case, the starting material Cu(SCN) reacted with 2-pic which exerts a strong super-conjugation effect from the CH_3 group to the pyridine ring which may result in 2-pic possessing a high tendency to coordinate with Cu atoms. The gradual dissolving of Cu(SCN) and the formation of the yellow solution were observed as evidence that the intermediate product, a single strand polymer $[(2\text{-pic})_2Cu(SCN)]_n$, had been prepared according to White *et al.*[23] Then the synthon tetrathiometalate $[MS_4]^{2-}$ acting as a bidentate ligand was added to the reaction system. The system immediately turned from yellow to black (or deep) red in color. Since the sequence of some Cu(I)-philic ligands of Mo(W)/S/Cu(Ag) clusters can be regarded as the following: S^{2-} > (py, 2-pic, PPh_3) > X^- (X = Cl, Br, I, CN), the former ligands can substitute some or all of the latter ligands, while the required coordination number of copper is not more than four. The single-strand polymer of the Cu complex might be separated into $(2\text{-pic})_2Cu(SCN)_2$-containing structural units, two bonds of which may be broken, both due to attack of the S^{2-} from the $[MS_4]^{2-}$ moiety. On the basis of our hypothesis, the probability of formation of the unit $[Cu(2\text{-pic})_2]$, $[Cu(2\text{-pic})(SCN)]$ and $[Cu(SCN)_2]$ are 1 : 2 : 1, which have a similar chance (1 : 2 : 1) to further coordinate with the $[MS_4]^{2-}$ moiety to form the final product with a symmetrical skeleton $[Et_4N]_2[MS_4Cu_4(SCN)_4(2\text{-pic})_4]$ (M = W **1**, Mo **2**).

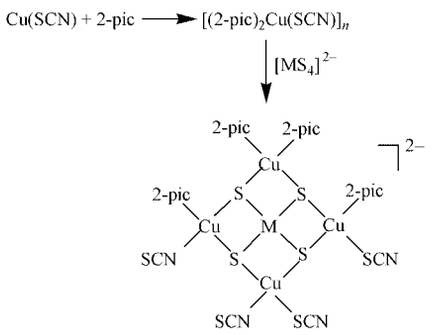

Table 2 Selected bond lengths (Å) and angles (°) of $[Et_4N]_2[WS_4Cu_4(SCN)_4(2\text{-pic})_4]$ **1**

W(1)–S(1A)	2.2379(11)	W(1)–S(2A)	2.2380(11)
W(1)–S(2)	2.2392(11)	W(1)–S(1)	2.2404(11)
Cu(1)–N(4)	1.975(5)	Cu(1)–N(1)	2.124(4)
Cu(2)–N(3)	1.996(4)	Cu(2)–N(3A)	1.998(4)
Cu(3)–N(2)	2.086(4)	Cu(3)–N(2A)	2.087(4)
Cu(1)–S(2)	2.3049(12)	Cu(1)–S(1A)	2.3301(11)
Cu(2)–S(2)	2.3091(11)	Cu(2)–S(2A)	2.3104(11)
Cu(3)–S(1)	2.3011(11)	Cu(3)–S(1A)	2.3037(11)
Cu(1A)–S(1)	2.3289(11)		
S(1A)–W(1)–S(2A)	110.29(4)	S(1A)–W(1)–S(2)	109.42(4)
S(2A)–W(1)–S(2)	108.63(6)	S(1A)–W(1)–S(1)	108.69(5)
S(2A)–W(1)–S(1)	109.45(4)	S(2)–W(1)–S(1)	110.36(4)
S(1A)–W(1)–Cu(3)	54.39(3)	S(2A)–W(1)–Cu(3)	125.66(3)
S(2)–W(1)–Cu(3)	125.71(3)	S(1)–W(1)–Cu(3)	54.30(3)
S(1A)–W(1)–Cu(1)	55.08(3)	S(2A)–W(1)–Cu(1)	127.28(3)
S(2)–W(1)–Cu(1)	54.40(3)	S(1)–W(1)–Cu(1)	123.28(3)
Cu(3)–W(1)–Cu(1)	88.863(12)	S(1A)–W(1)–Cu(1A)	123.22(3)
S(2A)–W(1)–Cu(1A)	54.47(3)	S(2)–W(1)–Cu(1A)	127.35(3)
S(1)–W(1)–Cu(1A)	55.02(3)	Cu(3)–W(1)–Cu(1A)	88.726(12)
Cu(1)–W(1)–Cu(1A)	177.59(2)	S(1A)–W(1)–Cu(2)	125.61(3)
S(2A)–W(1)–Cu(2)	54.34(3)	S(2)–W(1)–Cu(2)	54.29(3)
S(1)–W(1)–Cu(2)	125.70(3)	Cu(3)–W(1)–Cu(2)	180.000(9)
Cu(1)–W(1)–Cu(2)	91.137(12)	Cu(1A)–W(1)–Cu(2)	91.274(12)
N(4)–Cu(1)–N(1)	104.93(16)	N(4)–Cu(1)–S(2)	120.07(15)
N(1)–Cu(1)–S(2)	103.32(11)	N(4)–Cu(1)–S(1A)	108.37(13)
N(1)–Cu(1)–S(1A)	116.67(11)	S(2)–Cu(1)–S(1A)	104.08(4)
N(4)–Cu(1)–W(1)	133.39(13)	N(1)–Cu(1)–W(1)	121.68(11)
S(2)–Cu(1)–W(1)	52.17(3)	S(1A)–Cu(1)–W(1)	51.95(3)
N(3)–Cu(2)–N(3A)	104.2(3)	N(3)–Cu(2)–S(2)	105.26(12)
N(3A)–Cu(2)–S(2)	119.60(13)	N(3)–Cu(2)–S(2A)	119.58(13)
N(3A)–Cu(2)–S(2A)	105.33(12)	S(2)–Cu(2)–S(2A)	103.85(6)
N(3)–Cu(2)–W(1)	127.86(13)	N(3A)–Cu(2)–W(1)	127.93(13)
S(2)–Cu(2)–W(1)	51.95(3)	S(2A)–Cu(2)–W(1)	51.91(3)
N(2)–Cu(3)–N(2A)	108.4(2)	N(2)–Cu(3)–S(1)	111.48(12)
N(2A)–Cu(3)–S(1)	110.49(11)	N(2)–Cu(3)–S(1A)	110.51(11)
N(2A)–Cu(3)–S(1A)	111.54(12)	S(1)–Cu(3)–S(1A)	104.41(6)
N(2)–Cu(3)–W(1)	125.78(11)	N(2A)–Cu(3)–W(1)	125.82(11)
S(1)–Cu(3)–W(1)	52.25(3)	S(1A)–Cu(3)–W(1)	52.16(3)
W(1)–S(1)–Cu(3)	73.45(3)	W(1)–S(1)–Cu(1)	72.95(3)
Cu(3)–S(1)–Cu(1A)	110.28(4)	W(1)–S(2)–Cu(1)	73.43(3)
W(1)–S(2)–Cu(2)	73.76(3)	Cu(1)–S(2)–Cu(2)	114.93(5)

The clusters **1** and **2** were formed in an interesting mixed-ligand arrangement. Around the planar core structure of the $[MS_4Cu_4]$ aggregate, the two kinds of ligands were separately located in different parts of the structure, one kind of ligand (2-pic) was sited in the upper part of the cluster while the other was located in the lower part, exhibiting a novel pentanuclear 'open' py-derivative containing structure with an anion cluster core, which is reported for the first time. It is noticeable that the clusters **1** and **2** are partially different from those pentanuclear 'open' py-ligand containing clusters with the $[MS_4Cu_4]$ aggregate in a neutral structure, $[MS_4Cu_4X_2(py)_6]$ (X = Cl, Br, I, SCN),[5d,24] which were prepared by the following synthetic routes.

This difference in cluster structure between the present two clusters and those clusters, $[MS_4Cu_4X_2(py)_6]$, we have synthesized previously may be partially attributed to the fact that the coordination capability of 2-pic with Cu atoms is slightly weaker than py while that of SCN^- is a little stronger than X^- (X = Cl, Br, I, CN). These combined effects may give rise to the anion clusters containing four 2-pic ligands and four SCN ligands instead of six py ligands and two X ligands around the core structure.

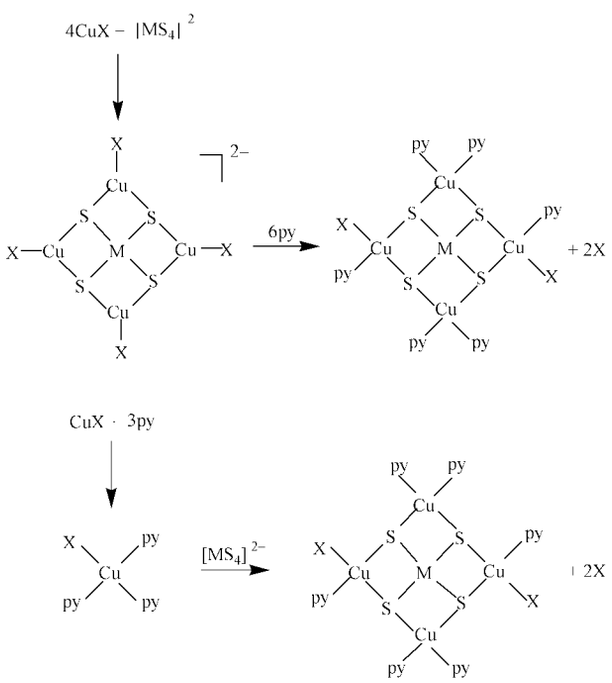

Crystal structure

Crystal structures of clusters **1** and **2** have been determined by X-ray diffraction. The structures of these two crystals consist of discrete $[Et_4N]^+$ cations and Mo(W)/S/Cu cluster anions. In both structures, the $[Et_4N]^+$ cations have their expected structure as well as normal distances and angles, which will not be discussed further. Selected bond distances and angles for **1** and **2** are collected in Tables 2 and 3 respectively.

The structure of the anion $[MS_4Cu_4(SCN)_4(2\text{-pic})_4]^{2-}$ in clusters **1** and **2** is shown in Figs. 1 and 2 respectively, and since these two structures are isomorphous, only the structure of

Table 3 Selected bond lengths (Å) and angles (°) of $[Et_4N]_2[MoS_4Cu_4(SCN)_4(2\text{-pic})_4]$ **2**

Mo(1)–S(2A)	2.237(2)	Mo(1)–S(2)	2.237(2)
Mo(1)–S(1A)	2.242(2)	Mo(1)–S(1)	2.242(2)
Cu(1)–N(4)	1.969(8)	Cu(1)–N(1)	2.133(7)
Cu(2)–N(3)	2.000(8)	Cu(2)–N(3A)	2.000(8)
Cu(3)–N(2)	2.086(7)	Cu(3)–N(2A)	2.086(7)
Cu(1)–S(2)	2.291(2)	Cu(1)–S(1A)	2.315(2)
Cu(2)–S(2)	2.295(2)	Cu(2)–S(2A)	2.296(2)
Cu(3)–S(1)	2.2900(19)	Cu(3)–S(1A)	2.2900(19)
Cu(1A)–S(1)	2.315(2)		
S(2A)–Mo(1)–S(2)	108.52(10)	S(2A)–Mo(1)–S(1A)	110.78(7)
S(2)–Mo(1)–S(1A)	109.15(7)	S(2A)–Mo(1)–S(1)	109.15(7)
S(2)–Mo(1)–S(1)	110.78(7)	S(1A)–Mo(1)–S(1)	108.46(10)
S(2A)–Mo(1)–Cu(3)	125.74(5)	S(2)–Mo(1)–Cu(3)	125.74(5)
S(1A)–Mo(1)–Cu(3)	54.23(5)	S(1)–Mo(1)–Cu(3)	54.23(5)
S(2A)–Mo(1)–Cu(1)	127.39(6)	S(2)–Mo(1)–Cu(1)	54.31(5)
S(1A)–Mo(1)–Cu(1)	54.89(5)	S(1)–Mo(1)–Cu(1)	123.46(5)
Cu(3)–Mo(1)–Cu(1)	88.84(3)	S(2A)–Mo(1)–Cu(1A)	54.31(5)
S(2)–Mo(1)–Cu(1A)	127.39(6)	S(1A)–Mo(1)–Cu(1A)	123.46(5)
S(1)–Mo(1)–Cu(1A)	54.89(5)	Cu(3)–Mo(1)–Cu(1A)	88.83(3)
Cu(1)–Mo(1)–Cu(1A)	177.67(6)	S(2A)–Mo(1)–Cu(2)	54.26(5)
S(2)–Mo(1)–Cu(2)	54.26(5)	S(1A)–Mo(1)–Cu(2)	125.77(5)
S(1)–Mo(1)–Cu(2)	125.77(5)	Cu(3)–Mo(1)–Cu(2)	180.0
Cu(1)–Mo(1)–Cu(2)	91.16(3)	Cu(1A)–Mo(1)–Cu(2)	91.17(3)
N(4)–Cu(1)–N(1)	104.6(3)	N(4)–Cu(1)–S(2)	119.5(2)
N(1)–Cu(1)–S(2)	103.1(2)	N(4)–Cu(1)–S(1A)	108.9(2)
N(1)–Cu(1)–S(1A)	116.4(2)	S(2)–Cu(1)–S(1A)	104.81(8)
N(4)–Cu(1)–Mo(1)	133.8(2)	N(1)–Cu(1)–Mo(1)	121.62(18)
S(2)–Cu(1)–Mo(1)	52.44(5)	S(1A)–Cu(1)–Mo(1)	52.41(5)
N(3)–Cu(2)–N(3A)	103.9(4)	N(3)–Cu(2)–S(2)	105.28(19)
N(3A)–Cu(2)–S(2)	119.4(2)	N(3)–Cu(2)–S(2A)	119.4(2)
N(3A)–Cu(2)–S(2A)	105.28(19)	S(2)–Cu(2)–S(2A)	104.53(11)
N(3)–Cu(2)–Mo(1)	128.0(2)	N(3A)–Cu(2)–Mo(1)	128.0(2)
S(2)–Cu(2)–Mo(1)	52.27(5)	S(2A)–Cu(2)–Mo(1)	52.26(5)
N(2)–Cu(3)–N(2A)	108.4(4)	N(2)–Cu(3)–S(1)	111.4(2)
N(2A)–Cu(3)–S(1)	110.20(18)	N(2)–Cu(3)–S(1A)	110.20(18)
N(2A)–Cu(3)–S(1A)	111.4(2)	S(1)–Cu(3)–S(1A)	105.20(11)
N(2)–Cu(3)–Mo(1)	125.78(19)	N(2A)–Cu(3)–Mo(1)	125.78(19)
S(1)–Cu(3)–Mo(1)	52.60(5)	S(1A)–Cu(3)–Mo(1)	52.60(5)
Mo(1)–S(1)–Cu(3)	73.17(6)	Mo(1)–S(1)–Cu(1A)	72.70(6)
Cu(3)–S(1)–Cu(1A)	110.41(8)	Mo(1)–S(2)–Cu(1)	73.25(6)
Mo(1)–S(2)–Cu(2)	73.48(6)	Cu(1)–S(2)–Cu(2)	114.90(9)

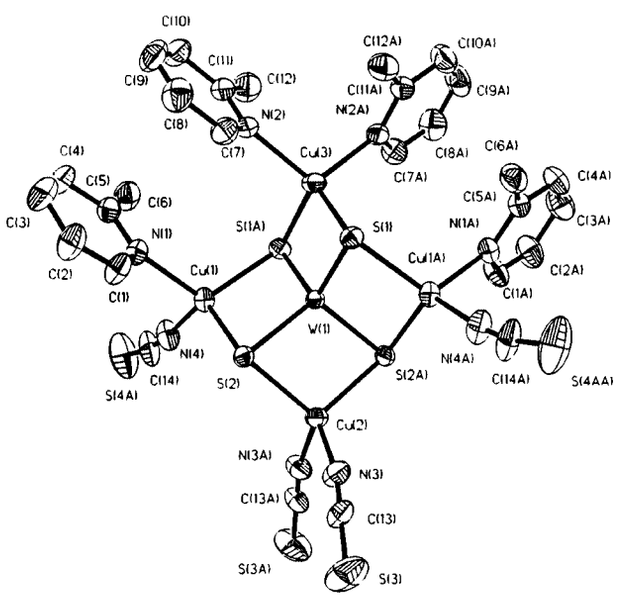

Fig. 1 A perspective view of the structure of anionic cluster $[Et_4N]_2[WS_4Cu_4(SCN)_4(2\text{-pic})_4]$ **1**.

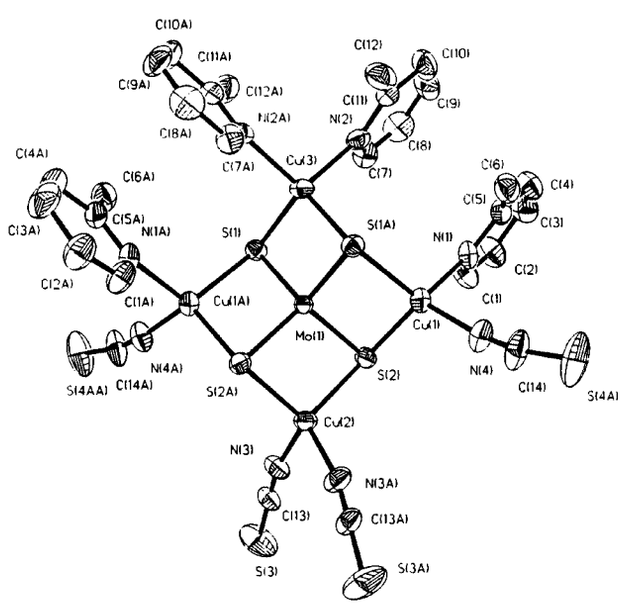

Fig. 2 A perspective view of the structure of anionic cluster $[Et_4N]_2[MoS_4Cu_4(SCN)_4(2\text{-pic})_4]$ **2**.

anion cluster **2** is described in detail. The anionic skeleton is composed of one Mo, four Cu and four μ_3-S atoms to form a MoS_4Cu_4 aggregate. The anion cluster contains a symmetry plane, passing through atoms Cu(3), Mo(1) and Cu(2) in which the Mo atom is in the center of the anion cluster while both the Mo and Cu atoms are essentially tetrahedrally coordinated. The two kinds of ligands (four 2-pic and four SCN^- ligands) are separately located on each side of the structure and result in the four Cu atoms being asymmetrically coordinated in three modes. Each of the two mutual *trans* Cu(1) and Cu(1A) atoms is bonded to two μ_3-S atoms, one 2-pic ligand and one SCN^-

group to form a distorted tetrahedral $S_2Cu(SCN)(2\text{-pic})$ unit. Atoms Cu(2) and Cu(3) are each coordinated by two μ_3-S atoms and either two 2-pic ligands or two SCN^- groups building up a distorted tetrahedral $[S_2Cu(2\text{-pic})_2$ or $S_2Cu(SCN)_2]$ unit respectively. The four Cu atoms with three kinds of coordination mode [one $S_2Cu(2\text{-pic})_2$ unit, one $S_2Cu(SCN)_2$ unit and a pair of $S_2Cu(SCN)(2\text{-pic})$ units] each ligate through two S atoms of one edge of the tetrahedral $[MoS_4]^{2-}$ moiety to construct the anionic cluster $[MoS_4Cu_4(SCN)_4(2\text{-pic})_4]^{2-}$. This arrangement with its anionic cluster core is quite different from the two general cases in 'open' structure pentanuclear clusters with py derivative as ligand: two kinds of coordination mode of Cu atoms in the neutral cluster $[MS_4Cu_4X_2(py)_6]$ (X = Cl, Br, I, SCN) and only one kind of that in the cationic cluster $[MS_4Cu_4(4\text{-pic})_8]^{2+}$.[25]

Owing to the three kinds of coordination modes of the Cu atoms, the four Cu–S bonds of cluster **2** are obviously different in length (2.290(1) in Cu(3)–S(1), 2.295(2) in Cu(2)–S(2), 2.315(2) in Cu(1)–S(1A) and 2.291(2) Å in Cu(1)–S(2)). It is noted that the Cu(1)–N(1) distance (2.133(7) Å) is longer than Cu(3)–N(2) (2.086(7) Å), while the Cu(1)–N(4) length (1.969(8) Å) is shorter than Cu(2)–N(3) (2.000(8) Å), and all of them compare with the average length of Cu–N (2.080(9) Å) in cluster $[MS_4Cu_4I_2(py)_6]$, which may demonstrate the influence of the three types of coordination mode of Cu atoms in this cluster structure. The N(2)–Cu(3)–N(2A) angle (108.4(4)°) is larger than the N(4)–Cu(1)–N(1) angle (104.6(3)°) and the N(3)–Cu(2)–N(3A) angle (103.9(4)°), while the N(2)–Cu(3)–S(1A) angle (110.20(18)°) is smaller than the N(1)–Cu(1)–S(1A) angle (116.4(2)°) and the N(4)–Cu(1)–S(2) angle (119.5(2)°) is bigger than the N(3)–Cu(2)–S(2A) angle (119.4(2)°). On the other hand, the different coordination modes of the Cu atoms also slightly influence the Mo–S bond lengths and the S–Mo–S angles, distance from the Mo atom to the four S atoms ranges from 2.237(2) to 2.242(2) Å, while the S–Mo–S angles change from 108.46(10) to 110.78(7)°. Although there are little differences in Mo–S bond lengths and S–Mo–S angles, they are still comparable to those observed in the clusters $[MS_4Cu_4X_2(py)_6]$ and $[MS_4Cu_4(4\text{-pic})_8](M_6O_{19})$, which suggests that the MoS_4 core still retains a tetrahedral coordinated geometry, the average length of the Mo–S bond (2.2395(2) Å) is 0.0615 Å longer than that of the original $[MoS_4]^{2-}$. Therefore, it is reasonable to believe that in the formation of cluster **2**, the Mo–S bonds weaken simultaneously with the formation of the Cu–S bonds. The angles Cu(3)–Mo(1)–Cu(2) and Cu(1)–Mo(1)–Cu(1A) are 180.0° and 177.67(6)° respectively, thus the anionic cluster structure is of pseudo D_{2d} symmetry and the five metal atoms are nearly coplanar with deviations of not more than 0.1 Å from the least-squares plane.

Infrared spectra and electronic spectra

The IR spectra of $[Et_4N]_2[MS_4Cu_4(SCN)_4(2\text{-pic})_4]$ exhibit characteristic strong bands at 439.8 cm^{-1} **1** and 450.6 cm^{-1} **2** assigned to the μ_3-S stretching vibration of the bridging MS_4 group, while the strong absorption peaks at 1602.5, 1482.9, 753.7 cm^{-1} **1** and 1602.7, 1483.1, 754.1 cm^{-1} **2** are typical vibration modes of the pyridine ring of 2-picoline, and the very strong absorption at 2087.9 cm^{-1} **1** and 2088.3 cm^{-1} **2** is attributed to the characteristic stretching vibration of the SCN^- group.

The UV-VIS absorption spectra of the clusters **1** and **2** in DMF are displayed in Fig. 3. It is noticed that the two clusters have very weak linear absorption at wavelengths ranging from 550 to 800 nm. The effective absorption bands at 286.5 nm for **2** and 426 nm for **1**, 507.5 nm for **2** are shown in the electronic spectra. The first strong band may be attributed to the charge transfer of the ligand to the Cu metal and another two absorptions can be assigned as charge-transfer bands of the type

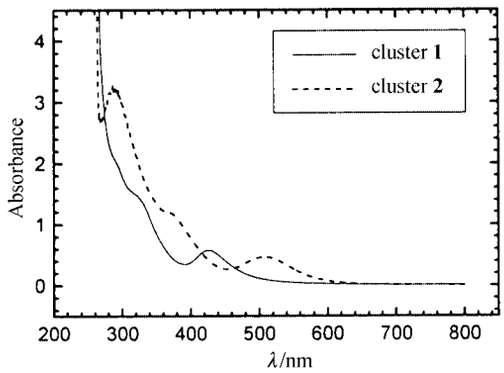

Fig. 3 Electronic spectra of $[Et_4N]_2[WS_4Cu_4(SCN)_4(2\text{-pic})_4]$ **1** and $[Et_4N]_2[MoS_4Cu_4(SCN)_4(2\text{-pic})_4]$ **2** in DMF solution with 1 cm optical path. The concentrations of **1** and **2** are 1.0×10^{-4} mol dm^{-3} respectively.

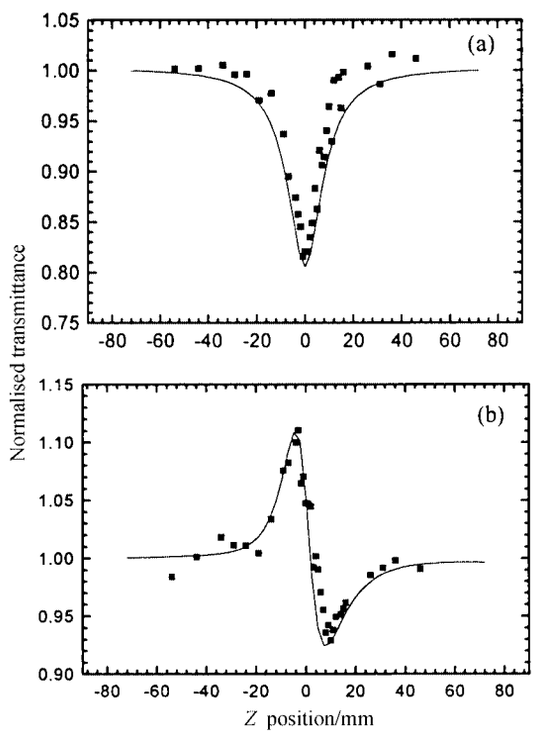

Fig. 4 *Z*-scan data of $[Et_4N]_2[WS_4Cu_4(SCN)_4(2\text{-pic})_4]$ in 6.98×10^{-4} mol dm^{-3} DMF solution at 532 nm with I_0 being 8.2×10^{12} W m^{-2}. (a) Collected under the open aperture configuration showing NLO absorption. (b) Obtained by dividing the normalized *Z*-scan data obtained under closed aperture configuration by the normalized *Z*-scan data in (a) (it shows the self-defocusing effect of the cluster **1**). The solid curves are the theoretical fit based on eqns. (1) and (2).

(π)S–(d)M (M = W, Mo) arising from the MS_4 moiety, which is red-shifted compared to the free $[MS_4]^{2-}$ anion (397 nm for W and 472 nm for Mo).

Nonlinear optical properties

The nonlinear optical (NLO) properties and the optical limiting (OL) performance of clusters **1** and **2** were investigated with 532 nm laser pulses of 8 ns duration in 6.98×10^{-4} mol dm^{-3} and 7.44×10^{-4}mol dm^{-3} DMF solutions for **1** and **2** respectively.

The nonlinear absorption components of clusters **1** and **2** were evaluated by *Z*-scan experiment under an open-aperture configuration (Fig. 4a, Fig. 5a). The NLO absorption data obtained under the conditions used in this study can be described by eqn. (1), which is derived to describe a third-order NLO absorptive process:

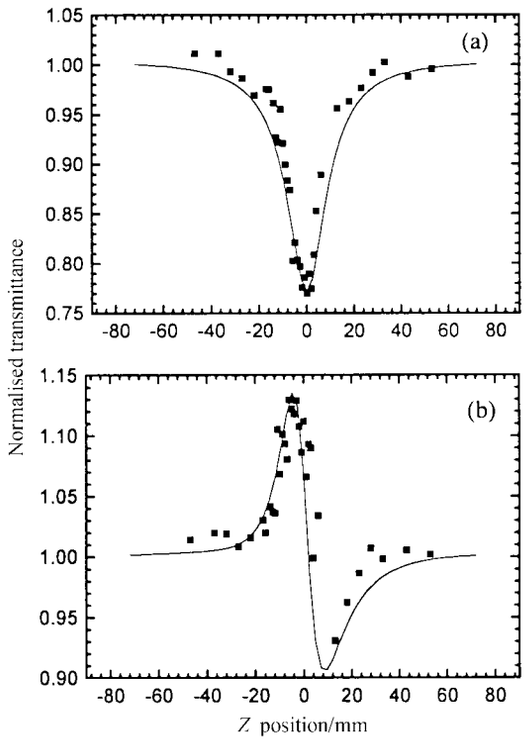

Fig. 5 Z-scan data of $[Et_4N]_2[MoS_4Cu_4(SCN)_4(2\text{-pic})_4]$ in 7.44×10^{-4} mol dm^{-3} DMF solution at 532 nm with I_0 being 8.2×10^{12} W m^{-2}. (a) Collected under the open aperture configuration showing NLO absorption. (b) Obtained by dividing the normalized Z-scan data obtained under closed aperture configuration by the normalized Z-scan data in (a) (it shows the self-defocusing effect of the cluster **2**). The solid curves are the theoretical fit based on eqns. (1) and (2).

$$T(Z) = \frac{1}{\sqrt{\pi}q(Z)} \int_{-\infty}^{\infty} \ln[1 + q(Z)]e^{-\tau^2} d\tau$$
$$q(Z) = a_2^{\text{eff}} I(Z) \frac{1 - e^{-a_0 L}}{a_0} \quad (1)$$

where a_0 and a_2 are linear and effective third-order NLO absorptive coefficients, L is the optical length and τ is the time. Light transmittance (T) is a function of the sample's Z-position (against focal point $Z = 0$).

The nonlinear refractive properties of clusters **1** and **2** were assessed by dividing the normalized Z-scan data obtained under the closed-aperture configuration by the normalized Z-scan data obtained under the open-aperture configuration (Fig. 4b, Fig. 5b). An effective third-order nonlinear refractive index n_2 can be derived from the difference between normalized transmittance values at valley and peak positions (ΔT_{v-p}) by eqn. (2) with measured values $\Delta T_{v-p} = -0.185$ **1** and -0.233 **2**.

$$n_2^{\text{eff}} = \frac{\lambda a_0}{0.812\pi I(1 - e^{-a_0 L})} \Delta T_{v-p} \quad (2)$$

A reasonably good fit between the experimental data and theoretical curve was obtained, which suggests that the experimentally obtained NLO effects are effectively third-order in nature. The effective a_2 values of 3.1×10^{-6} m W^{-1} **1**, 3.2×10^{-6} m W^{-1} **2** and n_2 values of -6.84×10^{-12} esu (esu = 7.162×10^{13} m^5 v^{-2}) **1**, -8.48×10^{-12} esu **2** respectively were derived for the samples from the theoretical curves. The excited state population (or absorption) can be responsible for these measured NLO effects. In accordance with the observed a_2 and n_2 values, the modulus of the effective third-order susceptibility $\chi^{(3)}$ can be calculated by eqn. (3) where ν is the frequency of the laser light. For 6.98×10^{-4} mol dm^{-3} **1** and 7.44×10^{-4} mol dm^{-3} **2** in DMF

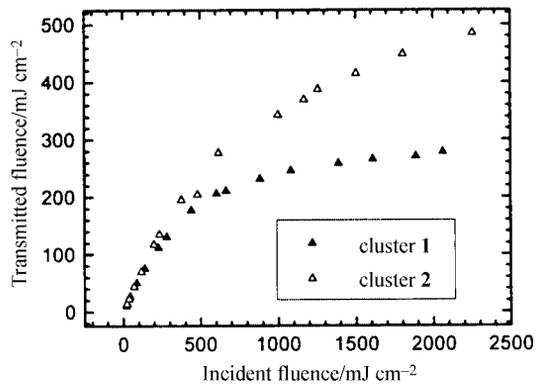

Fig. 6 Optical limiting effect of $[Et_4N]_2[WS_4Cu_4(SCN)_4(2\text{-pic})_4]$ **1** (6.98×10^{-4} mol dm^{-3} in DMF) and $[Et_4N]_2[MoS_4Cu_4(SCN)_4(2\text{-pic})_4]$ **2** (7.44×10^{-4} mol dm^{-3} in DMF).

$$|\chi^{(3)}| = \sqrt{\left(\left| \frac{9 \times 10^8 \varepsilon_0 n_0^2 c^2}{2\nu} a_2 \right|^2 + \left| \frac{cn_0^2}{80\pi} n_2 \right|^2 \right)} \quad (3)$$

solution, the $\chi^{(3)}$ values were calculated to be 6.5×10^{-8} **1** and 8.9×10^{-8} esu **2**. The corresponding modulus of the hyperpolarizabilities γ of 9.42×10^{-32} esu **1** and 1.29×10^{-31} esu **2** were obtained from $\chi^{(3)} = \gamma N F^4$, where N is the number density (concentration) of the clusters in the samples; $F^4 = 3$ is the local field correction factor.

From the discussions above, we can reasonably state that clusters **1** and **2** have similar NLO properties. Both exhibit strong self-defocusing performance and reverse saturable absorption (RSA) as displayed in Fig. 4 and Fig. 5. Their NLO refractive properties and NLO absorptive properties (RSA) may be comparable to the combined behavior of the nest-shaped clusters and the cubane-like shaped clusters, which typically show strong self-defocusing and RSA effects respectively.

The presence of the combined effects of strong RSA and self-defocusing in clusters **1** and **2** may significantly enhance the overall optical limiting (OL) performance of these two clusters. The optical limiting (OL) effects of cluster **1** and **2** are depicted in Fig. 6. It manifests that at very low fluence they respond linearly to the incident fluence obeying Beer's law. The light transmittance starts to deviate from Beer's law of the linear response when the input light fluence rises to certain values with respect to each cluster, and the solution becomes increasingly less transparent. The values of the limiting threshold are measured as 0.3 J cm^{-2} and 0.5 J cm^{-2} for clusters **1** and **2** respectively from the OL experimental data.

Table 4 lists a few heterothiometallic clusters with their limiting thresholds. From the perspective of the OL application, the present two clusters with pentanuclear 'open' structure are comparable to (or slightly better than) the known good optical limiting materials: cubane-like shaped clusters. Within a limited number of series of clusters where both the W- and Mo-containing clusters are measured, such a comparison can be made. The W-containing clusters seem always able to outperform their corresponding Mo-containing counterparts in OL performance at a given wavelength and with similar linear transmittance. This is consistent with the case that the OL effects of Ag-containing clusters are better than their Cu-containing homologs, which may be due to the heavy-atom effect. This very fact strongly implies that heterothiometallic clusters may be designed and synthesized to obtain predictable and controllable NLO properties.

Acknowledgements

This project was supported by the National Science Foundation (No. 29631040) and the Malaysian Government and Universiti

Table 4 The limiting thresholds of compounds measured at 532 nm with ns laser pulses

Compound	Structure	Solvent	Linear transmission (%)	Limiting threshold/J cm^{-2}	Ref.
$[NBu_4]_3[WS_4Cu_3Br_4]$	Cubane-like shaped	MeCN	70	1.3	5(*a*)
$[NBu_4]_3[WS_4Ag_3Br_4]$	Cubane-like shaped	MeCN	70	0.6	5(*a*)
$[Bu_4N]_3[MoS_4Ag_3BrI_3]$	Cubane-like shaped	MeCN	70	0.5	2(*a*)
$[NBu_4]_3[MoS_4Ag_3Br_4]$	Cubane-like shaped	MeCN	72	0.7	2(*a*)
$[NBu_4]_3[MoS_4Ag_3BrCl_3]$	Cubane-like shaped	MeCN	70	0.6	2(*a*)
$[NBu_4]_2[MoOS_3Cu_3(NCS)_3]$	Nest shaped	MeCN	71	7	5(*c*)
$[NBu_4]_2[MoOS_3Cu_3BrCl_2]$	Nest shaped	MeCN	73	10	12(*b*)
$[Et_4N]_4[Mo_2O_2S_6Cu_6Br_2I_4]$	Twin-nest shaped	MeCN	70	2	11(*b*)
$[MoOS_3Cu_3(PPh_3)_3\{S_2P(OBu)_2\}]$	Open cubane-like shaped	CH_2Cl_2	90	5	14(*b*)
$[MoS_4Ag_3(PPh_3)_3\{S_2P(OBu)_2\}]$	Open cubane-like shaped	CH_2Cl_2	90	0.8	14(*b*)
$[MoS_4Cu_6I_4(py)_4]_n$	Two-dimensional network	DMSO		0.6	19
$[Mo_2Ag_4S_8(PPh_3)_4]$	Hexagonal-prism shaped	MeCN	92	0.1	5(*b*)
$[Et_4N]_2[MoS_4Cu_4(SCN)_4(2\text{-pic})_4]$	Planar 'open' shaped	DMF	84	0.5	This work
$[Et_4N]_2[WS_4Cu_4(SCN)_4(2\text{-pic})_4]$	Planar 'open' shaped	DMF	86	0.3	This work

Sains Malaysia for research grant R&D No. 190-9609-2801. S. S. S. R. thanks Universiti Sains Malaysia for a Visiting Post-Doctoral Fellowship.

References

1 (*a*) *Conference on Lasers and Electro-Optics*, 1993, OSA Technical Digest Series, vol. 11, Optical Society of America, Washington, DC, 1993, p. 614; (*b*) S. R. Marder, J. E. Sohn and G. D. Stucky, *Materials for Nonlinear Optics-Chemical Perspectives*, American Chemical Society, Washington, DC, 1991, p. 455; (*c*) J. L. Bredas, C. Adant, P. Tackx, A. Persoons and B. M. Pierce, *Chem. Rev.*, 1994, **94**, 243.

2 (*a*) S. Shi, W. Ji, S. H. Tang, J. P. Lang and X. Q. Xin, *J. Am. Chem. Soc.*, 1994, **116**, 3615; (*b*) E. W. Van Stryland, Y. Y. Wu, D. J. Hagan, M. J. Soilean and K. Mansour, *J. Opt. Soc. Am. B*, 1988, **5**, 1980; (*c*) T. J. Bunning, L. V. Natarajan, M. G. Schmitt, B. L. Epling and L. R. Crane, *Appl. Opt.*, 1991, **30**, 4341.

3 (*a*) L. W. Tutt and A. Kost, *Nature* (*London*), 1992, **356**, 225; (*b*) D. G. McLean, R. L. Sutherland, M. C. Brant, D. M. Brandelik, P. A. Fleitz and T. Pottenger, *Opt. Lett.*, 1993, **18**, 858; (*c*) A. Kost, L. W. Tutt, M. B. Klein, T. K. Dougherty and W. E. Elias, *Opt. Lett.*, 1993, **18**, 334.

4 (*a*) J. W. Perry, K. Mansour, I. Y. S. Lee, X. L. Wu, P. V. Bedworth, C. T. Chen, D. Ng, S. R. Marder, P. Miles, T. Wada, M. Tian and H. Sasabe, *Science*, 1996, **273**, 1553; (*b*) T. H. Wei, D. J. Hagan, M. J. Sence, E. W. Van Stryland, J. W. Perry and D. R. Coulter, *Appl. Phys. B*, 1992, **54**, 46; (*c*) S. Banerjee, G. R. Kumar, P. Mathur and P. Sekar, *Chem. Commun.*, 1997, 299.

5 (*a*) S. Shi, W. Ji, J. P. Lang and X. Q. Xin, *J. Phys. Chem.*, 1994, **98**, 3570; (*b*) W. Ji, S. Shi, H. J. Du, P. Ge, S. H. Tang and X. Q. Xin, *J. Phys. Chem.*, 1995, **99**, 17297; (*c*) S. Shi, W. Ji, W. Xie, T. C. Chong, H. C. Zeng, J. P. Lang and X. Q. Xin, *Mater. Chem. Phys.*, 1995, **39**, 298; (*d*) K. M. L. Michael, H. W. Hou, H. G. Zheng, W. T. Wang, G. X. Jin, X. Q. Xin and W. Ji, *Chem. Commun.*, 1998, 505; (*e*) T. Xia, A. Dogariu, K. Mansour, D. J. Hagan, A. A. Said, E. W. Van Stryland and S. Shi, *J. Opt. Soc. Am. B*, 1998, **15**, 1497.

6 C. R. Giuliano and L. D. Hess, *IEEE J. Quantum Electron.*, 1967, 358.

7 J. W. Perry, K. Mansour, S. R. Marder, K. J. Perry, J. D. Alvarez and I. Choong, *Opt. Lett.*, 1994, **19**, 625.

8 L. W. Tutt and S. W. McCahon, *Opt. Lett.*, 1990, **15**, 700.

9 R. Signorini, M. Zerbetto, M. Meneghetti, R. Bozio, M. Maggini, C. D. Faveri, M. Prato and G. Scorrano, *Chem. Commun.*, 1996, 1891.

10 G. R. Allan, D. R. Labergerie, S. J. Rychnovsky, T. F. Boggess, A. L. Smirl and L. W. Tutt, *J. Phys. Chem.*, 1992, **96**, 6313.

11 (*a*) H. W. Hou, D. L. Long, X. Q. Xin, X. Y. Huang, B. S. Kang, P. Ge, W. Ji and S. Shi, *Inorg. Chem.*, 1996, **35**, 5363; (*b*) H. W. Hou, X. Q. Xin, J. Liu, M. Q. Chen and S. Shi, *J. Chem. Soc.*, *Dalton Trans.*, 1994, 3211.

12 (*a*) P. Ge, S. H. Tang, W. Ji, S. Shi, H. W. Hou, D. L. Long, X. Q. Xin, S. F. Lu and Q. J. Wu, *J. Phys. Chem. B*, 1997, **101**, 27; (*b*) H. W. Hou, X. R. Ye, X. Q. Xin, J. Liu, M. Q. Chen and S. Shi, *Chem. Mater.*, 1995, **7**, 472.

13 (*a*) Z. R. Chen, H. W. Hou, X. Q. Xin, K. B. Yu and S. Shi, *J. Phys. Chem.*, 1995, **99**, 8717; (*b*) H. W. Hou, B. Liang, X. Q. Xin, K. B. Yu, P. Ge, W. Ji and S. Shi, *J. Chem. Soc.*, *Faraday Trans.*, 1996, **92**, 2343; (*c*) S. Shi, Z. R. Chen, H. W. Hou, X. Q. Xin and K. B. Yu, *Chem. Mater.*, 1995, **7**, 1519.

14 (*a*) P. E. Hoggard, H. W. Hou, X. Q. Xin and S. Shi, *Chem. Mater.*, 1996, **8**, 2218; (*b*) D. L. Long, S. Shi, X. Q. Xin, B. S. Luo, L. R. Chen, X. Y. Huang and B. S. Kang, *J. Chem. Soc.*, *Dalton Trans.*, 1996, 2617; (*c*) W. Ji, H. J. Du, S. H. Tang and S. Shi, *J. Opt. Soc. Am. B*, 1995, **12**, 876; (*d*) D. X. Zeng, W. Ji, W. T. Wong, W. Y. Wong and X. Q. Xin, *Inorg. Chim. Acta*, 1998, **279**, 172.

15 S. Shi, W. Ji and X. Q. Xin, *J. Phys. Chem.*, 1995, **99**, 894.

16 G. Salane, T. Shibahara, H. W. Hou, X. Q. Xin and S. Shi, *Inorg. Chem.*, 1995, **34**, 4785.

17 S. Shi, H. W. Hou and X. Q. Xin, *J. Phys. Chem.*, 1995, **99**, 4050.

18 H. G. Zheng, W. Ji, M. K. M. Low, G. Sakane, T. Shibahara and X. Q. Xin, *J. Chem. Soc.*, *Dalton Trans.*, 1997, 2357.

19 H. W. Hou, Y. T. Fan, C. X. Du, Y. Zhu, W. L. Wang, X. Q. Xin, M. K. M. Low, W. Ji and H. G. Ang, *Chem. Commun.*, 1999, 647.

20 J. W. McDonald, G. D. Frieson, L. D. Rosenhein and W. E. Newton, *Inorg. Chim. Acta*, 1983, **72**, 205.

21 M. Kabesova, M. Dunaj-Jurco, M. Serator and J. Gazo, *Inorg. Chim. Acta*, 1976, **17**, 161.

22 G. M. Sheldrick, SHELXTL-PC (version 5.1), Siemens Analytical Instruments, Inc., Madison, WI, 1997.

23 (*a*) N. K. Mills and A. H. White, *J. Chem. Soc.*, *Dalton Trans.*, 1984, 229; (*b*) P. C. Healy, C. Pakawatchai, R. I. Papasergio, V. A. Patrick and A. H. White, *Inorg. Chem.*, 1984, **23**, 3769; (*c*) C. L. Raston, B. Walter and A. H. White, *Aust. J. Chem.*, 1979, **32**, 2757.

24 C. Zhang, Y. L. Song, G. C. Jin, G. Y. Fang, Y. X. Wang, S. S. Raj, H. K. Fun and X. Q. Xin, unpublished work.

25 M. T. Pope, J. P. Lang, X. Q. Xin and K. B. Yu, *Chin. J. Chem.*, 1995, **13**, 40.